

Geophysical Research Letters[®]



RESEARCH LETTER

10.1029/2023GL104987

Key Points:

- Nitrous oxide (N₂O) undersaturation in inland waters is prevalent, indicating that inland waters periodically act as sinks of atmospheric N₂O
- Periodic N₂O sink behavior occurs at most monitored sites and the frequency of N₂O sink behavior is invariant to ecosystem size or biome
- N₂O sink behavior has the strong potential to partially offset N₂O emissions from inland waters

Supporting Information:

Supporting Information may be found in the online version of this article.

Correspondence to:

K. S. Aho,
kellyaho@msu.edu

Citation:

Aho, K. S., Maavara, T., Cawley, K. M., & Raymond, P. A. (2023). Inland waters can act as nitrous oxide sinks: Observation and modeling reveal that nitrous oxide undersaturation may partially offset emissions. *Geophysical Research Letters*, 50, e2023GL104987. <https://doi.org/10.1029/2023GL104987>

Received 21 JUN 2023
Accepted 16 OCT 2023

Inland Waters can Act as Nitrous Oxide Sinks: Observation and Modeling Reveal that Nitrous Oxide Undersaturation May Partially Offset Emissions

K. S. Aho^{1,2} , T. Maavara³ , K. M. Cawley¹, and P. A. Raymond⁴ 

¹National Ecological Observatory Network, Battelle, Boulder, CO, USA, ²Department of Earth and Environmental Science, Department of Integrative Biology, Michigan State University, East Lansing, MI, USA, ³School of Geography, University of Leeds, Leeds, UK, ⁴School of the Environment, Yale University, New Haven, CT, USA

Abstract Inland waters are significant, yet highly uncertain, natural sources of nitrous oxide (N₂O). Many emission models assume that N₂O is only emitted from freshwaters, and that N₂O sink behavior is negligible. However, observational studies have reported N₂O undersaturation, suggesting that inland waters can act as N₂O sinks due to net N₂O consumption. This study leverages data from the National Ecological Observatory Network (NEON) and an existing global emission model to examine the prevalence of and controls on N₂O undersaturation in streams, rivers, and lakes across scales and biomes. We find that N₂O undersaturation is prevalent in the NEON data set (14%–30% of samples) and process-based model outputs (38%), occurring across biomes and spatial scales. Failing to account for undersaturation in the NEON data set could result in a 100% overestimation of N₂O emissions. These results show that consideration of N₂O sink behavior is needed for accurate emission estimates.

Plain Language Summary Nitrous oxide (N₂O) is a climate-relevant greenhouse gas that is increasing in the atmosphere due to human activities. It also contributes to stratospheric ozone depletion. Inland waters (e.g., streams, rivers, and lakes) are significant, yet uncertain, sources of N₂O to the atmosphere. In general, emission models assume that N₂O is produced in and emitted from inland waters. However, field observations have shown that inland waters can also act as sinks of atmospheric N₂O, potentially offsetting emissions. Understanding when and where inland waters act as N₂O sinks is needed for accurate emission estimates. This study uses a large observational data set and an existing global emission model to explore when, where, and to what extent inland waters act as N₂O sinks. The results show that N₂O sink behavior is common and may significantly offset emissions.

1. Introduction

Nitrous oxide (N₂O) is a potent and long-lasting greenhouse gas that contributes to ozone depletion (Canadell et al., 2021; Ravishankara et al., 2009). Inland waters (e.g., streams, rivers, and lakes) are significant, yet highly uncertain, natural sources of N₂O to the atmosphere (e.g., Hu et al., 2016; Seitzinger & Kroeze, 1998; Zheng et al., 2022). The general assumption is that N₂O emissions from inland waters increase with reactive nitrogen inputs and nitrogen transformation rates (Maavara et al., 2019; Marzadri et al., 2017; Yao et al., 2020). However, field observation has shown that inland waters can also act as N₂O sinks, even when appreciable levels of reactive nitrogen are present (Aho et al., 2022; Soued et al., 2016; Webb et al., 2019). These field observations have generally been treated as unique situations, and there has not been a large-scale assessment of the extent of N₂O sink behavior in inland waters.

Source versus sink behavior is driven by the N₂O concentration gradient between the atmosphere and the water. In other words, inland waters emit N₂O when dissolved N₂O concentrations are greater than the atmospheric equilibrium N₂O concentration (“oversaturated”) and are sinks of atmospheric N₂O when dissolved N₂O concentrations are less than the atmospheric equilibrium N₂O concentration (“undersaturated”). Oversaturation occurs when N₂O production outpaces N₂O consumption, and undersaturation occurs when consumption outpaces production. Because air-water gas exchange continuously pushes the concentration gradient towards equilibrium, sustained over- or undersaturation indicates that net production or consumption rates outpace air-water diffusion rates.

© 2023. The Authors.

This is an open access article under the terms of the [Creative Commons Attribution License](https://creativecommons.org/licenses/by/4.0/), which permits use, distribution and reproduction in any medium, provided the original work is properly cited.

The net balance of N₂O production and consumption processes depends on various microbially mediated transformations of reactive nitrogen (Quick et al., 2019). The net balance of these processes is difficult to predict because N₂O is a byproduct or intermediate of these reactive nitrogen transformations, rather than the end-product. For example, denitrification can both produce and consume N₂O, because N₂O is an intermediate of nitrate reduction via denitrification: NO₃⁻ → NO₂⁻ → NO → N₂O → N₂. In other words, incomplete denitrification produces N₂O but complete denitrification can consume N₂O. Nitrous oxide is also produced during other nitrogen transformations. For example, N₂O is produced as a byproduct of nitrate reduction via dissimilatory nitrate reduction to ammonium (Stevens & Laughlin, 1998) and ammonia oxidation via both nitrification (Yoshida & Alexander, 1970) and nitrifier denitrification (Goreau et al., 1980). In general, denitrification and nitrification are considered to be the dominant transformations controlling N₂O concentrations in inland waters (Maavara et al., 2019; Mwanake et al., 2019; Seitzinger & Kroeze, 1998). Furthermore, the rate of N₂O equilibration across the air-water boundary varies greatly across and within aquatic ecosystems (Klaus & Vachon, 2020; Raymond et al., 2012; Ulseth et al., 2019), adding a physical control to the various of biological controls that impact the degree of N₂O saturation.

The objective of this study is to explore the prevalence of N₂O undersaturation in inland waters. This study leverages (a) observational data from 34 stream, river, and lakes monitored by the National Ecological Observatory Network (NEON) and (b) an existing global process-based model of N₂O emissions from inland waters (Maavara et al., 2019). The observational data from NEON provides a unique opportunity to explore N₂O undersaturation across a broad range of aquatic ecosystems, including streams, rivers, and lakes in temperate, tropical, and boreal biomes. The process-based model complements the NEON observational data by providing a mechanistic understanding of the environmental conditions that support N₂O undersaturation more broadly. Together, these two approaches show that N₂O undersaturation can be prevalent in inland waters under some environmental and climatic conditions, and N₂O sink behavior may partially offset emissions.

2. Data and Methods

2.1. NEON Sites

This study includes 34 aquatic sites in the National Ecological Observatory Network (NEON). These sites comprise seven lakes, three non-wadable rivers, and 24 wadable streams located across the United States, from Alaska to Puerto Rico (Figure 1). Site descriptions (Tables S1 and S2 in Supporting Information S1) show that these sites generally represent inland waters across scales and biomes, although overall these sites are not highly developed. Sites range from small streams to large rivers: Walker Branch (WALK) in Tennessee is the smallest stream with a 1.1 km² drainage basin and the Lower Tombigbee River (TOMB) in Alabama is the largest river, draining 47,000 km². NEON sites were distributed across the United States according to statistically partitioned eco-climatic domains (Hargrove & Hoffman, 2004) to capture ecologically variability across the United States. Therefore, sites also span latitudes and biomes: Rio Cupeyes (CUPE) in Puerto Rico is the southernmost lotic site and Oksrukuyik Creek (OKSR) in northern Alaska is the northernmost. Lakes also span both sizes and latitudes. Prairie Pothole (PRPO) in North Dakota is the smallest lake; Lake Barco (BARC) in Florida is the southernmost lake; and Toolik Lake (TOOK) in Alaska is both the largest and northernmost lake. In sum, NEON sites capture a large swath of inland-water types across the United States.

2.2. NEON Data and Data Treatment

This study leverages dissolved N₂O concentration data from the NEON dissolved gases in surface water data product (DPI.20097.001), which has been previously processed and released (Aho et al., 2021). NEON collects headspace equilibration samples by hand ~26 or ~12 times per year at lotic and lentic sites, respectively, and publishes raw mixing ratios for both the equilibrated headspace and atmospheric samples. NEON started data collection at each site between 2014 and 2018; depending on the site, between 1.5 and 6 years of data is available. Aho et al. (2021) calculated in situ dissolved N₂O concentrations from the air and headspace mixing ratios provided by NEON, adjusted for sample and water temperature and barometric pressure. The average coefficient of variation of field triplicates was 17%. The processing scripts are available at <https://github.com/kellyaho/NEON-GHG-processing>, and full documentation and inputs files are available with the derived data product on the Environmental Data Initiative (Aho et al., 2021). This study only considers surface water samples (i.e., NEON

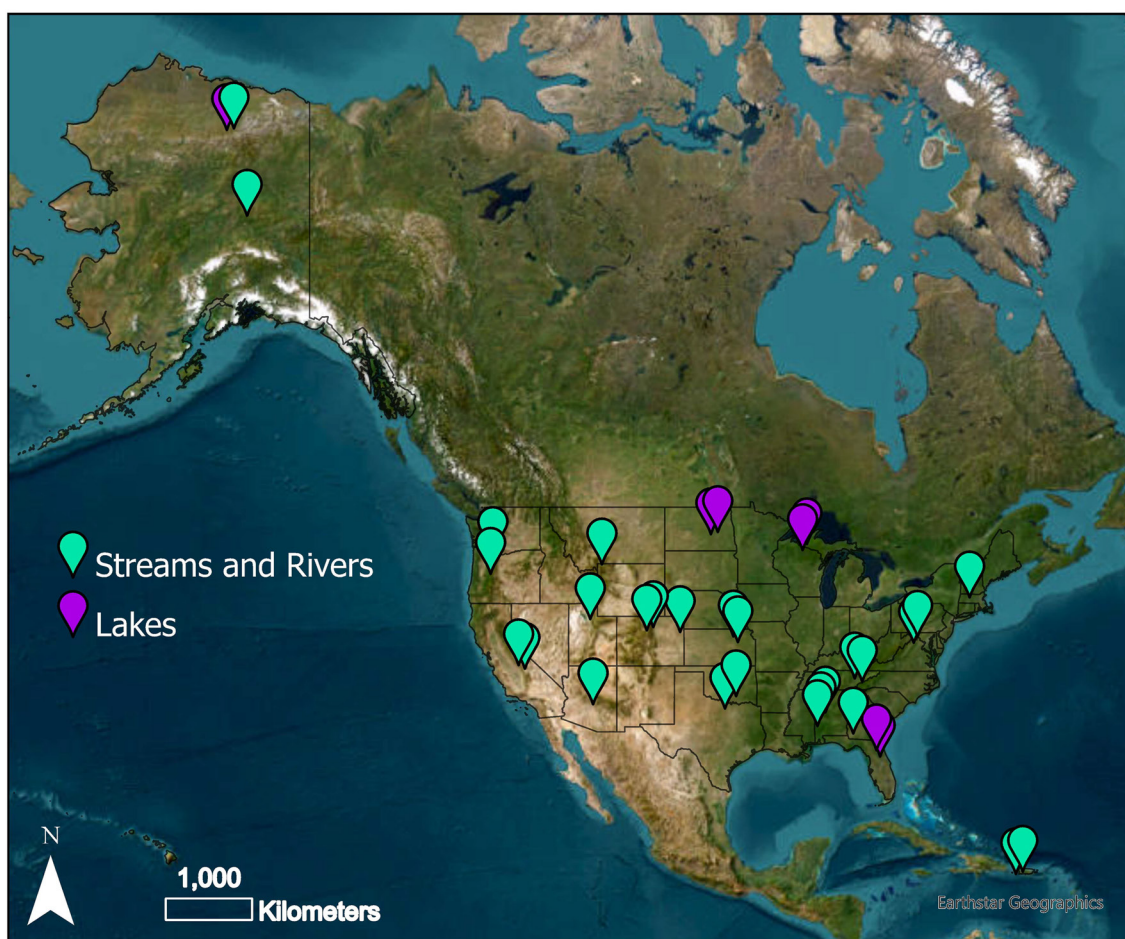


Figure 1. Map of NEON aquatic sites across the United States. A jitter is used to offset closely placed sites. Please see Tables S1 and S2 in Supporting Information S1 for complete site descriptions, including coordinates.

codes SS, C0, and C1) and paired air samples. Table S5 in Supporting Information S1 provides further details on the treatment and processing of NEON data.

N_2O fluxes were calculated from the air-water N_2O concentration gradient and gas transfer velocity (k_{N_2O}). Gas transfer velocity was calculated according to Klaus and Vachon (2020) for lakes and Raymond et al. (2012) for streams and rivers. For lakes, the normalized gas transfer velocity (k_{600}) was calculated from lake surface area and wind speed (Klaus & Vachon, 2020). Surface area was estimated from Google Maps satellite imagery and wind speed at 10 m was calculated from the NEON wind speed data product (DP1.20059.001) and vertical position using the `wind.scale.base()` function in LakeMetabolizer (Winslow et al., 2016). For streams and rivers, k_{600} was calculated from water velocity and streambed slope (Equation 4 in Raymond et al., 2012). Water velocity was calculated from the NEON instantaneous discharge data product (DP4.00130.001) using site-specific hydraulic geometry relationships (Figure S8 in Supporting Information S1). Slope was collected from NEON thalweg surveys (DP4.00131.001) for all sites, except for BLWA, FLNT, and TOMB; slope for these sites were taken from the United State Geological Survey's High Resolution National Hydrography Dataset Plus (NHDPlus HR). Finally, for both lentic and lotic sites, k_{600} was converted to k_{N_2O} with temperature-dependent Schmidt numbers (Wanninkhof, 1992). Table S5 in Supporting Information S1 provides further detail.

Ancillary parameters, such as other nitrogen species (i.e., nitrate, ammonium, total dissolved nitrogen), phosphorus (i.e., total phosphorus, orthophosphorus), and dissolved organic carbon, are from the NEON Chemical properties of surface water data product (DP1.20093.001). Measurements of pH were not reliable during the 2014–2020 study timeframe (<https://www.neonscience.org/impact/observatory-blog/uncertainty-ph-measurements>). Therefore, in this study, pH was calculated from dissolved inorganic carbon concentration and the partial

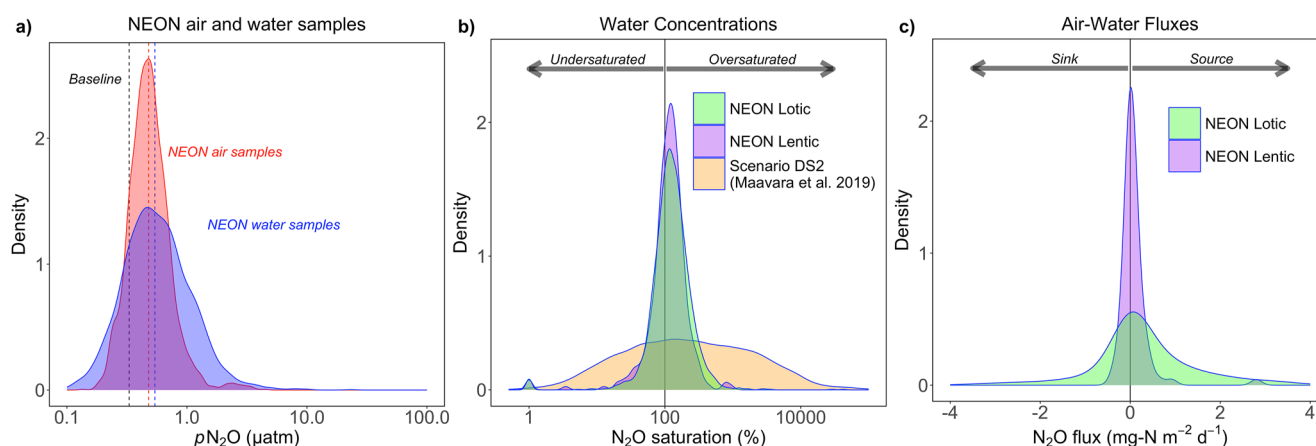


Figure 2. Density plots of (a) all NEON air and water pN_2O samples, with vertical lines marking the global “baseline” pN_2O value from over marine surfaces (0.33 μatm ; CSIRO, 2021; Lan et al., 2023), the median NEON air pN_2O value (0.48 μatm), and the median NEON water pN_2O value (0.54 μatm); (b) water N_2O concentrations given in terms of saturation for all NEON samples and for all process-based model outputs (Maavara et al., 2019); and (c) N_2O flux rates calculated from NEON water samples.

pressure of carbon dioxide (Figure S9 in Supporting Information S1). More details about NEON data products and processing are summarized in Table S5 in Supporting Information S1.

This analysis focuses on N_2O saturation, or the ratio of dissolved N_2O concentration and the concentration of dissolved N_2O if the water was in equilibrium. The degree of saturation therefore depends, not only on the dissolved N_2O concentration in water, but also on the atmospheric concentration used for comparison. Previous studies have calculated N_2O saturation in two ways: (a) using paired air samples (e.g., Clough et al., 2011; Cole & Caraco, 2001; Soued et al., 2016) and (b) using a global over-ocean mean (Aho et al., 2022; Baulch et al., 2011; Borges et al., 2019; Webb et al., 2019). In this study, we leverage the extensive set of paired air samples in the NEON data set; calculating saturation from paired air samples, adjusted for solubility according to Henry’s Law constants (Sander, 2015). However, the air pN_2O values from NEON are variable and higher than global over-ocean values (CSIRO, 2021; Lan et al., 2023) for the same timeframe (Figure 2a; 0.54 ± 0.32 vs. 0.33 μatm ; Figure S1 in Supporting Information S1). In addition, there is a weak positive relationship between air pN_2O and paired water pN_2O values (Figure S2a in Supporting Information S1; $R^2 = 0.15$, $p < 0.01$), which may reflect higher near-surface N_2O concentrations in areas where aquatic concentrations are higher or sample carry over during analysis. Also, there is a weak negative relationship between air pN_2O values and the paired water N_2O saturation (Figure S2b in Supporting Information S1; $R^2 = 0.11$), indicating a correlation between aquatic N_2O undersaturation and these higher air samples. In this analysis, we choose to leverage the paired air samples. However, because these higher atmospheric values are more associated with instances of undersaturation than using a constant value of 0.33 μatm , we also present saturation compared to a global over-ocean value of 0.33 μatm in the text.

Aquatic N_2O saturation levels were classified as undersaturated (<95%), ~atmospheric equilibrium (95%–105%), and oversaturated (>105%). The distribution of saturation levels was assessed with density and violin plots. Site-specific averages for N_2O saturation and flux were calculated and compared; simple averaging was chosen because NEON collects samples at approximately the same intervals throughout the year using the same protocols, which minimizes sampling biases. Linear regression was used to assess predictors of N_2O undersaturation frequency in both the NEON data set and the model outputs.

Mixed-effects models were used to identify environmental drivers of N_2O saturation in the NEON data. Due to the nested structure of the NEON data set (i.e., repeat sampling at individual sites), site was used as a random effect using the lmer() function from the lmer4 R package (version 1.1–34). We tested the following predictor variables based on the literature (e.g., Quick et al., 2019; Soued et al., 2016; Webb et al., 2019): stream discharge, water temperature, k_{600} , pH, dissolved oxygen, nitrate + nitrite, ammonium, total dissolved nitrogen, total phosphorus, orthophosphorus, the ratio of orthophosphorus to total dissolved nitrogen (i.e., proxy for nitrogen or phosphorus limitation), dissolved organic carbon, and iron. We selected the best model with the anova() R function, which

considers Akaike's information criterion (AIC) and the Bayesian information criterion (BIC). All data analysis was completed in R version 4.2.3 (R Core Team, 2023).

2.3. Process-Based Model

To generalize the results from the NEON data set, the outputs of rerunning an existing global process-based model that predicts N_2O emissions for lentic and lotic environments were also considered (Lauerwald et al., 2019; Maavara et al., 2019). Specifically, the mechanistic box model portion of Maavara et al. (2019)'s model was used because it predicts hypothetical N_2O concentrations for a large combination of freshwater nitrogen dynamics using a Monte Carlo approach. The box model includes pools for nitrate, ammonium, dissolved organic nitrogen, particulate organic nitrogen, and N_2O , including all influxes and effluxes into and from the water body for each of these species, and major transformations and loss terms for each of these species. Probability density functions (PDFs) were constrained from literature data and available databases to reflect the global distribution of annual-scale water body hydrological and physical parameters (e.g., water residence time, flow, volume, surface area) and rate constants (mainly first order). Full details regarding how the PDFs were constrained and how the box model was structured can be found in Maavara et al. (2019).

The model was originally constrained to represent annual average emissions rates for whole open water bodies (i.e., whole reservoirs, lakes, river reaches, and estuaries). This approach therefore artificially distributes emissions equally across all unit volumes of water within the water body and across the entire year, rather than identifying hotspots and hot moments where we might expect the emissions to occur (e.g., during the growing season). To aid interpretation, we have converted to denitrification and nitrification rates to $nmol\ l^{-1}\ hr^{-1}$ but emphasize that these results represent spatiotemporally averaged values.

In Maavara et al. (2019), multiple scenarios are used to calculate the N_2O emissions flux; in this paper, however, this study uses only "Default Scenario 2" (DS2), which is the only scenario that explicitly calculates N_2O concentrations in a water body, allowing for production of N_2O via nitrification, and both production and consumption of N_2O via denitrification, with the extent dependent on the water residence time and available nitrate and ammonium. Saturation is calculated compared to an air value of $0.33\ \mu atm$. In Maavara et al. (2019), the authors were only interested in calculating N_2O emissions from inland water bodies, and so water bodies with N_2O undersaturation were not included in the upscaling of the Monte Carlo output to global watersheds. Here, we rerun the model's Monte Carlo approach to generate a theoretically "globally representative" hypothetical database of nitrogen and N_2O dynamics, and retain all N_2O concentrations generated, including undersaturated values.

3. Results and Discussion

3.1. N_2O Concentrations at NEON Aquatic Sites

On average, NEON aquatic sites were slightly supersaturated with N_2O compared to the atmosphere (Figure 2). The mean \pm standard deviation pN_2O is $0.84 \pm 4.20\ \mu atm$ for streams and rivers and $0.60 \pm 0.42\ \mu atm$ for lakes, compared to $0.54 \pm 0.32\ \mu atm$ for near-surface atmospheric samples (Figure 2a). These values correspond to a mean \pm standard deviation N_2O saturation was $184 \pm 1,081\%$ for streams and rivers, and $133 \pm 94\%$ for lakes when using paired air samples (Figure 2b). If a constant $0.33\text{-}\mu atm$ air value was used instead, N_2O saturation would be $272 \pm 1,400\%$ for streams and rivers and $193 \pm 129\%$ for lakes. For streams and rivers, King's Creek (KING), a headwater stream in Kansas, had the lowest mean N_2O saturation compared to paired air samples ($100 \pm 49\%$) and Sycamore Creek (SYCA), an intermittent stream in Arizona, had by far the highest mean N_2O saturation ($1,850 \pm 7,541\%$; Table S3 in Supporting Information S1). For lakes, Prairie Pothole (PRPO), a small prairie lake in North Dakota, had the lowest mean N_2O saturation compared to paired air samples, approximately at atmospheric equilibrium ($103 \pm 53\%$), and Little Rock Lake (LIRO), a small temperate lake in Wisconsin, had the highest ($150 \pm 124\%$; Table S3 in Supporting Information S1).

3.2. N_2O Undersaturation Is Common in the NEON Data Set

Although NEON sites were, on average, supersaturated with N_2O , there were many instances of undersaturation. Here, we consider N_2O saturation of less than 95% as undersaturated; between 95% and 105% as approximately in equilibrium with the atmosphere; and greater than 105% as supersaturated. An appreciable number of samples

were undersaturated: compared to paired air samples, 30% of lotic samples (678 of 2,288; Figure 2b) and 32% of lentic samples (97 of 306; Figure 2b). When compared to a constant 0.33- μatm air value instead of paired air samples, 15% of lotic samples and 11% of lentic samples were undersaturated. It is notable that all 34 NEON sites experienced N_2O undersaturation to some extent compared to paired air samples, from 6% of samples from Flint River (FLNT), a large river draining 15,000 km^2 in Georgia, to 72% of samples from Upper Big Creek (BIGC), a small river draining 11 km^2 in the Sierra Nevada mountains in California (Figure 3). Compared to 0.33- μatm , all NEON sites experienced N_2O undersaturation at some point, except for the Blue River (BLUE), a large prairie stream in Oklahoma. Interestingly, the prevalence of N_2O undersaturation does not change with latitude (Figure S3a in Supporting Information S1), ecosystem size (Figure S3b in Supporting Information S1), or slope for lotic sites ($p > 0.05$). Other studies have reported N_2O undersaturation in individual ecosystems, including boreal streams and lakes (Soued et al., 2016), a wetland-draining stream (Baulch et al., 2011), and the Congo watershed (Borges et al., 2019; Upstill-Goddard et al., 2017). However, this analysis is unique by finding that N_2O undersaturation is a widespread phenomenon, occurring at almost all sites monitored by NEON. In other words, this study extends previous field-scale studies by generalizing the report of N_2O undersaturation at all sites across spatial scales, biomes, and ecosystem type.

Because N_2O undersaturation is temporally emergent at almost all NEON sites, within-site monitoring is likely responsible for detecting its somewhat irregular occurrence. NEON's monitoring approach (i.e., ~ 26 or ~ 12 samples per year at lotic and lentic sites, respectively) is important for detecting N_2O undersaturation as there is a temporal component to its occurrence. For example, in temperate and boreal streams and rivers, undersaturation occurs more frequently outside of the growing season (Figures S4 and S5 in Supporting Information S1). Further, mixed-effect models show that water temperature is positively related to N_2O saturation across all lotic sites (estimate \pm standard error: 0.03 ± 0.003), indicating seasonality in temperate and boreal ecosystems. Lakes, however, do not exhibit similar seasonality (Figures S4 and S5 in Supporting Information S1) and relationships between saturation and lake temperature are insignificant (estimate \pm standard error: -0.003 ± 0.005). The apparent lack of seasonality in lake N_2O saturation may be due to interactions with lake stratification dynamics, as stratification has been reported as a control on N_2O dynamics (Webb et al., 2019). However, it is more difficult to draw widespread conclusions given the fewer samples collected at lentic sites compared to lotic sites. Interestingly, even at lotic sites exhibiting seasonality, interannual variability can be high (Figure S6 in Supporting Information S1). For example, in Como Creek, a mountain stream in Colorado exhibiting seasonality in N_2O saturation across years (Figure S5 in Supporting Information S1), 48% of samples were undersaturated in 2017 compared to 4% of samples in 2019. This type of interannual variability in the occurrence of N_2O undersaturation has been previously reported in a temperate watershed (Aho et al., 2022). This analysis of NEON data shows that interannual variability in undersaturation is a widespread occurrence and that temporal patterns in N_2O undersaturation are far from uniform across years.

3.3. NEON Aquatic Sites Act as Temporary N_2O Sinks

The direction of air-water gas flux is determined by the air-water concentration gradient. Therefore, when a waterbody is undersaturated with nitrous oxide compared to the atmosphere, that waterbody acts as a sink of atmospheric N_2O . Although the mean N_2O diffusive flux rate to the atmosphere across the NEON data set was positive, negative fluxes were prevalent and notably offset emission rates (Figure 2c). The average diffusive flux rate was $1.04 \pm 5.71 \text{ mg-N m}^{-2} \text{ d}^{-1}$ for streams and rivers, and $0.09 \pm 0.37 \text{ mg-N m}^{-2} \text{ d}^{-1}$ for lakes (Figure 2c). These mean rates fall within ranges reported by recent literature reviews for streams and rivers (-0.14 – $58.83 \text{ mg-N m}^{-2} \text{ d}^{-1}$, Zhang et al., 2022) and for lakes and impounded water (-0.22 – $5.77 \text{ mg-N m}^{-2} \text{ d}^{-1}$, DelSontro et al., 2018), respectively. The NEON data set allows for consideration of the importance of negative flux rates. If negative flux rates in the NEON data set were ignored, the average diffusive flux rate would double for streams and rivers ($2.08 \pm 6.81 \text{ mg-N m}^{-2} \text{ d}^{-1}$) and more than double for lakes ($0.20 \pm 0.43 \text{ mg-N m}^{-2} \text{ d}^{-1}$), highlighting the role of N_2O undersaturation in offsetting total N_2O emissions. In other words, inland waters can act as N_2O sinks frequently enough that consideration of negative fluxes is important to avoid overestimating N_2O emissions from inland waters.

The spatial coverage of the NEON data set is unique and provides insights into where aquatic ecosystems act as N_2O sinks most frequently (Table S4 in Supporting Information S1). One of the 27 NEON stream and river sites had a negative mean flux rate (Upper Big Creek, CA [BIGC], $-0.26 \pm 0.94 \text{ mg-N m}^{-2} \text{ d}^{-1}$), and two of the

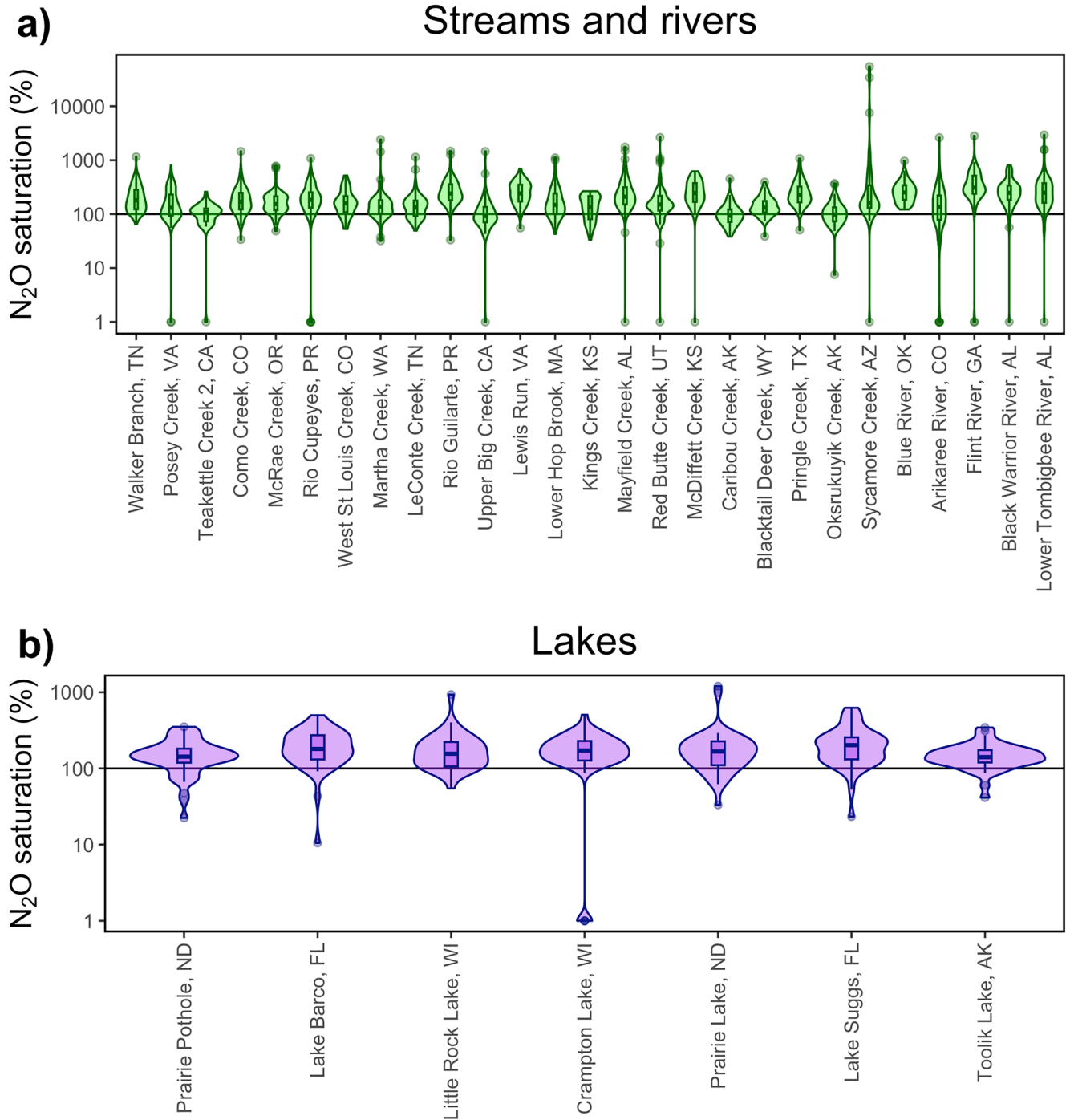


Figure 3. Violin plots with embedded boxplots of N_2O saturation compared to paired air samples for (a) NEON stream and river sites and (b) NEON lake sites. Boxes represent the median and interquartile range (IQR), whiskers mark the lesser of $1.5 \times IQR$ or minimum/maximum, and points denote outliers more extreme than $1.5 \times IQR$. A saturation of 100% implies atmospheric equilibrium and is noted with a horizontal line. Sites are arranged from left to right in order of watershed area for lotic ecosystems and surface area for lentic ecosystems.

seven lakes had negative mean flux rates (Toolik Lake, AK [TOOK], $-0.26 \text{ mg-N m}^{-2} \text{ d}^{-1}$ and Prairie Pothole, ND [PRPO], $-0.09 \pm 0.07 \text{ mg-N m}^{-2} \text{ d}^{-1}$). In addition, other sites were essentially neutral, as negative fluxes offset positive fluxes (Black Warrior River, AL [BLWA], $0 \pm 0.01 \text{ mg-N m}^{-2} \text{ d}^{-1}$; King's Creek, KS [KING], $0 \pm 0.02 \text{ mg-N m}^{-2} \text{ d}^{-1}$; and Lower Tombigbee River, AL [TOMB], $0.01 \pm 0.02 \text{ mg-N m}^{-2} \text{ d}^{-1}$). Interestingly, these sites with negative or neutral flux rates were diverse in size (e.g., spanning from the smallest to the largest

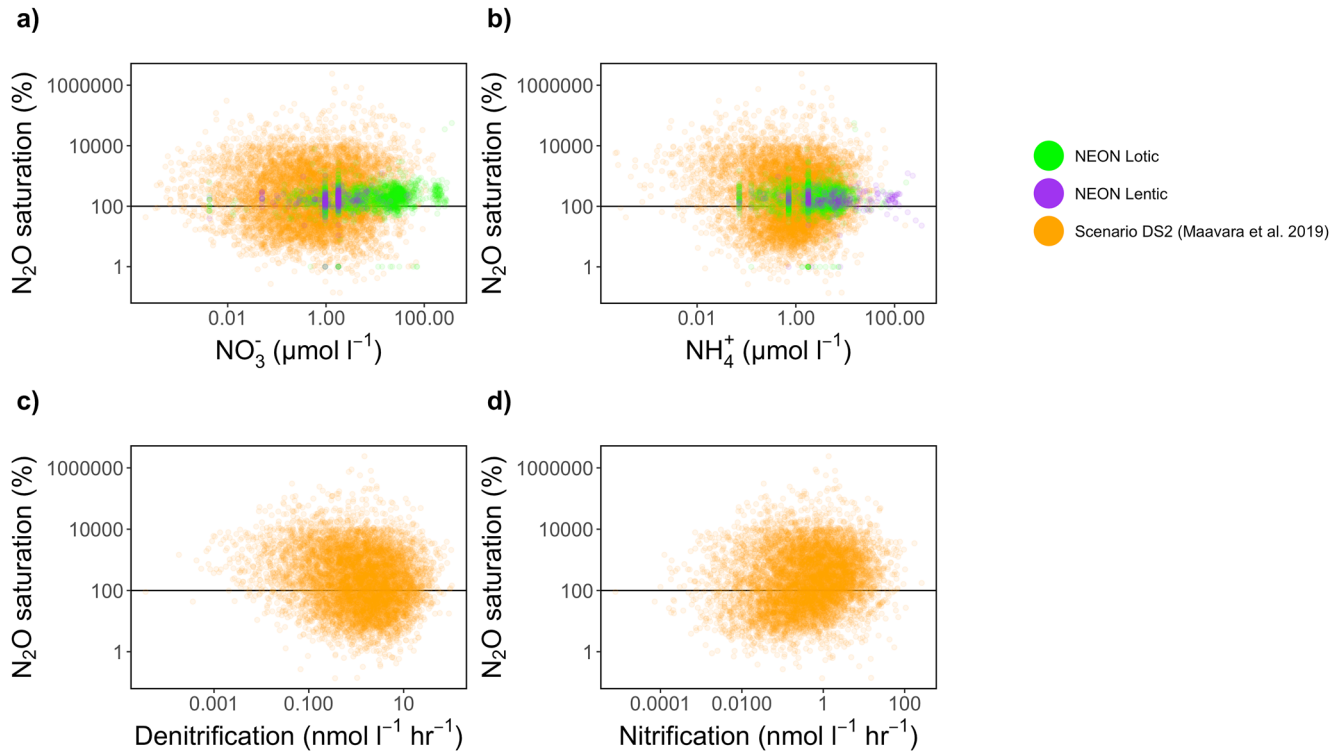


Figure 4. Relationships between N_2O saturation and (a) NO_3^- , (b) NH_4^+ , (c) denitrification rate, and (d) nitrification rate. For all subplots, model outputs from rerunning Maavara et al. (2019)'s process-based model using scenario DS2 are shown in orange. In subplots (a) and (b), these outputs are overlaid with NEON field data from lotic sites in green and lentic sites in purple.

systems) and location (e.g., spanning from boreal and mountain to prairie and subtropical biomes), indicating that varied aquatic ecosystems can experience N_2O undersaturation significant enough to offset emissions.

3.4. Drivers of N_2O Undersaturation and Sink Behavior

We use a process-based model to contextualize and generalize NEON field observations. Rerunning Maavara et al. (2019)'s DS2 scenario outputs a similar percentage of undersaturated samples (38%) as occurs in the NEON data set. However, the Maavara et al. (2019) global model outputs have a wider distribution than the NEON data, reflecting the broader range of inputs to the model compared to those of the 34 NEON aquatic sites (Figure 2b). This generalization allows us to consider the mechanisms that support N_2O undersaturation, beyond what is possible from field observation alone (Figure 4). Overall, model outputs indicate that N_2O saturation increases with rates of denitrification and nitrification (Figures 4c and 4d), regardless of DIN availability (Figures 4a and 4b). In other words, low levels of denitrification and nitrification seem to support the occurrence of N_2O undersaturation.

This study can only hypothesize on why low levels of nitrogen transformation support N_2O undersaturation. The occurrence of N_2O undersaturation indicates that the rate of N_2O consumption outpaces the rate of N_2O production. Low rates of denitrification and nitrification may support N_2O undersaturation through two related mechanisms: (a) low N_2O production rates due to limited nitrogen transformation and (b) complete denitrification of N_2O produced. In other words, our results suggest that, at low nitrogen transformation rates, complete denitrification likely supports the reduction of N_2O from both incomplete denitrification, as well as from other sources (i.e., nitrification, atmospheric invasion). Undersaturation implies that consumption processes, likely the complete denitrification of N_2O to N_2 , outpaces not only N_2O production processes by also invasion of atmospheric N_2O across the air-water boundary.

The NEON data also supports the finding that N_2O undersaturation is associated with low levels of nitrogen transformation, at least in streams and rivers (Table 1). A mixed-effect model for lotic NEON sites shows that

Table 1
Mixed-Effects Model for Predicting N₂O Saturation in Lotic Systems From the NEON Observational Data

Model	Variable	Estimate	SE
log(N ₂ O saturation) ~ Water Temp × NO ₃ ⁻ + NO ₂ ⁻ + pH + (1 site)	Intercept	4.951	0.521
	Water Temp	0.031	0.003
	NO ₃ ⁻ + NO ₂ ⁻	0.049	0.090
	pH	-0.617	0.066
	Water Temp × NO ₃ ⁻ + NO ₂ ⁻	0.021	0.005

water temperature (estimate ± std error: 0.03 ± 0.003) and the interaction between water temperature and nitrate + nitrite (NO₃⁻ + NO₂⁻) concentration (0.02 ± 0.005) are positively correlated with N₂O saturation, while pH (-0.62 ± 0.067) is negatively correlated. The first two conditions associated with low N₂O saturation (low temperature, simultaneous low temperature and low NO₃⁻ + NO₂⁻) suggest that low denitrification rates may promote net N₂O consumption. In general, warmer temperatures are associated with increased rates of various microbial processes, like denitrification (McCutchan & Lewis, 2008; Velthuis & Veraart, 2022) and nitrification (Starry et al., 2005). Further, in agreement with our results, lower temperature has been associated with lower N₂O concentrations in streams and rivers (Beaulieu et al., 2010; Gardner et al., 2016, but see Baulch et al., 2011). In terms of substrate for denitrification, NO₃⁻ + NO₂⁻ levels alone are insignificant in predicting N₂O saturation (0.05 ± 0.090), but the interaction between water temperature and NO₃⁻ + NO₂⁻ concentrations is significant (0.02 ± 0.005, Figure S10 in Supporting Information S1). In other words, N₂O saturation increases with NO₃⁻ + NO₂⁻ concentration, only under warmer conditions. This finding agrees with previous work suggesting that substrate availability alone does not promote high rates of denitrification, but rather that both substrate availability and environmental conditions that encourage denitrification are required (Maavara et al., 2019; Marzadri et al., 2017). The final condition associated with low N₂O saturation (high pH) may suggest the balance between N₂O production and consumption when denitrification occurs. Previous work has shown that low pH can inhibit nitrous oxide reductase (Knowles, 1982), indicating that perhaps elevated pH allows for N₂O consumption via N₂O reduction to N₂ gas. For NEON lentic sites, no environmental variables were significant predictors of N₂O saturation, perhaps because there are fewer lentic samples than lotic samples.

4. Conclusions

In conclusion, both an existing model (Lauerwald et al., 2019; Maavara et al., 2019) and NEON observational data show that inland waters experience appreciable levels of N₂O undersaturation. In fact, NEON data shows that N₂O undersaturation is temporally emergent at almost all monitored sites, suggesting that its occurrence is widespread. Overall, N₂O undersaturation seems to occur when rates of nitrogen transformation are low and our results suggest that, under certain conditions, complete denitrification can consume N₂O from, not only incomplete denitrification, but also other nitrogen transformations and atmospheric invasion. It is worth noting that, in general, NEON aquatic sites are not highly impacted by human activity and so similar prevalence of N₂O undersaturation is not expected in highly developed areas. However, the prevalence of N₂O undersaturation indicates that N₂O sink behavior may partially offset positive emissions and should be considered in emission estimates.

Data Availability Statement

All data used are publicly available from the Environmental Data Initiative and NEON. Specifically, the following data were used:

Dissolved greenhouse gas concentrations derived from the NEON dissolved gases in surface water data product (DP1.20097.001) are available at Aho et al. (2021).

NEON Dissolved gases in surface water (DP1.20097.001), RELEASE-2021 is available at NEON (2021).

NEON Barometric pressure (DP1.00004.001), RELEASE-2022 is available at NEON (2022a).

NEON Chemical properties of surface water (DP1.20093.001), RELEASE-2022 is available at NEON (2022b).

NEON Continuous discharge (DP4.00130.001), RELEASE-2022 is available at NEON (2022c).
 NEON Reaeration field and lab collection (DP1.20190.001), RELEASE-2022 is available at NEON (2022d).
 NEON Stream morphology map (DP4.00131.001), RELEASE-2022 is available at NEON (2022e).
 NEON Temperature at specific depth in surface water (DP1.20264.001), RELEASE-2022 is available at NEON (2022f).
 Temperature (PRT) in surface water (DP1.20053.001), RELEASE-2022 is available at NEON (2022g).
 NEON Water quality (DP1.20288.001), RELEASE-2022 is available at NEON (2022h).
 NEON Windspeed and direction above water on-buoy (DP1.20059.001), RELEASE-2022 is available at NEON (2022i).
 In addition, the NEON greenhouse gas processing scripts are available at <https://github.com/kellyaho/NEON-GHG-processing> and permanently archived at Aho (2023).

Acknowledgments

This research was supported by K.A.'s postdoctoral fellowship at the National Ecological Observatory Network.

References

- Aho, K. S. (2023). kellyaho/NEON-GHG-processing: Version 1 (v1.0) [Software]. Zenodo. <https://doi.org/10.5281/zenodo.8386776>
- Aho, K. S., Cawley, K., DelVecchia, A., Stanley, E., & Raymond, P. (2021). Dissolved greenhouse gas concentrations derived from the NEON dissolved gases in surface water data product (DP1.20097.001) [Dataset]. Environmental Data Initiative. <https://doi.org/10.6073/pasta/47d7cb6d374b6662cce98e42122169f8>
- Aho, K. S., Fair, J. H., Hosen, J. D., Kyzivat, E. D., Logozzo, L. A., Weber, L. C., et al. (2022). An intense precipitation event causes a temperate forested drainage network to shift from N₂O source to sink. *Limnology & Oceanography*, 67(S1), 1–16. <https://doi.org/10.1002/lno.12006>
- Baulch, H. M., Schiff, S. L., Maranger, R., & Dillon, P. J. (2011). Nitrogen enrichment and the emission of nitrous oxide from streams. *Global Biogeochemical Cycles*, 25(4). <https://doi.org/10.1029/2011GB004047>
- Beaulieu, J. J., Shuster, W. D., & Rebholz, J. A. (2010). Nitrous oxide emissions from a large, impounded river: The Ohio river. *Environmental Science and Technology*, 44(19), 7527–7533. <https://doi.org/10.1021/es1016735>
- Borges, A. V., Darchambeau, F., Lambert, T., Morana, C., Allen, G. H., Tambwe, E., et al. (2019). Variations in dissolved greenhouse gases (CO₂, CH₄, N₂O) in the Congo River network overwhelmingly driven by fluvial-wetland connectivity. *Biogeosciences*, 16(19), 3801–3834. <https://doi.org/10.5194/bg-16-3801-2019>
- Canadell, J. G., Monteiro, P. M. S., Costa, M. H., da Cunha, L. C., Cox, P. M., Eliseev, A. V., et al. (2021). 2021: Global carbon and other biogeochemical cycles and feedbacks. In V. Masson-Delmotte (Ed.), *Climate change 2021: The physical science basis. contribution of working Group I to the sixth assessment report of the intergovernmental panel on climate change*. Cambridge University Press/Cambridge. <https://doi.org/10.1017/9781009157896.007>
- Clough, T. J., Buckthought, L. E., Casciotti, K. L., Kelliher, F. M., & Jones, P. K. (2011). Nitrous oxide dynamics in a Braided river system, New Zealand. *Journal of Environmental Quality*, 40(5), 1532–1541. <https://doi.org/10.2134/jeq2010.0527>
- Cole, J. J., & Caraco, N. F. (2001). Emissions of nitrous oxide (N₂O) from a tidal, freshwater river, the Hudson River, New York. *Environmental Science and Technology*, 35(6), 991–996. <https://doi.org/10.1021/es0015848>
- CSIRO. (2021). Cape grim N₂O data.
- DelSontro, T., Beaulieu, J. J., & Downing, J. A. (2018). Greenhouse gas emissions from lakes and impoundments: Upscaling in the face of global change. *Limnology and Oceanography Letters*, 3(3), 64–75. <https://doi.org/10.1002/lol2.10073>
- Gardner, J. R., Fisher, T. R., Jordan, T. E., & Knee, K. L. (2016). Balancing watershed nitrogen budgets: Accounting for biogenic gases in streams. *Biogeochemistry*, 127(2–3), 231–253. <https://doi.org/10.1007/s10533-015-0177-1>
- Goreau, T. J., Kaplan, W. A., Wofsy, S. C., McElroy, M. B., Valois, F. W., & Watson, S. W. (1980). Production of NO₂⁻ and N₂O by nitrifying bacteria at reduced concentrations of oxygen. *Applied and Environmental Microbiology*, 40(3), 526–532. <https://doi.org/10.1128/aem.40.3.526-532.1980>
- Hargrove, W. W., & Hoffman, F. M. (2004). Potential of multivariate quantitative methods for delineation and visualization of ecoregions. *Environmental Management*, 34(S1), S39–S60. <https://doi.org/10.1007/s00267-003-1084-0>
- Hu, M., Chen, D., & Dahlgren, R. A. (2016). Modeling nitrous oxide emission from rivers: A global assessment. *Global Change Biology*, 22(11), 3566–3582. <https://doi.org/10.1111/gcb.13351>
- Klaus, M., & Vachon, D. (2020). Challenges of predicting gas transfer velocity from wind measurements over global lakes. *Aquatic Sciences*, 82(3), 1–17. <https://doi.org/10.1007/s00027-020-00729-9>
- Knowles, R. (1982). Denitrification. *Microbiological Reviews*, 46(1), 43–70. <https://doi.org/10.1128/mr.46.1.43-70.1982>
- Lan, X., Thoning, K. W., & Dlugokencky, E. J. (2023). Trends in globally-averaged CH₄, N₂O, and SF₆ determined from NOAA global monitoring laboratory measurements, 2023.05. <https://doi.org/10.15138/P8XG-AA10e>
- Lauerwald, R., Regnier, P., Figueiredo, V., Enrich-Prast, A., Bastviken, D., Lehner, B., et al. (2019). Natural lakes are a minor global source of N₂O to the atmosphere. *Global Biogeochemical Cycles*, 33(12), 1564–1581. <https://doi.org/10.1029/2019GB006261>
- Maavara, T., Lauerwald, R., Laruelle, G. G., Akbarzadeh, Z., Bouskill, N. J., Van Cappellen, P., & Regnier, P. (2019). Nitrous oxide emissions from inland waters: Are IPCC estimates too high? *Global Change Biology*, 25(2), 473–488. <https://doi.org/10.1111/gcb.14504>
- Marzadri, A., Dee, M. M., Tonina, D., Bellin, A., & Tank, J. L. (2017). Role of surface and subsurface processes in scaling N₂O emissions along riverine networks. *Proceedings of the National Academy of Sciences*, 114(17), 4330–4335. <https://doi.org/10.1073/pnas.1617454114>
- McCutchan, J. H., & Lewis, W. M. (2008). Spatial and temporal patterns of denitrification in an effluent-dominated plains river. *SIL Proceedings*, 1922-2010, 30(2), 323–328. <https://doi.org/10.1080/03680770.2008.11902136>
- Mwanake, R. M., Gettel, G. M., Aho, K. S., Namwaya, D. W., Masese, F. O., Butterbach-Bahl, K., & Raymond, P. A. (2019). Land use, not stream order, controls N₂O concentration and flux in the Upper Mara River Basin, Kenya. *Journal of Geophysical Research: Biogeosciences*, 124(11), 3491–3506. <https://doi.org/10.1029/2019JG005063>

- NEON (National Ecological Observatory Network). (2021). Dissolved gases in surface water (DP1.20097.001), RELEASE-2021 [Dataset]. NEON Data Portal. <https://doi.org/10.48443/fb19-g348>
- NEON (National Ecological Observatory Network). (2022a). Barometric pressure (DP1.00004.001) RELEASE-2022 [Dataset]. NEON Data Portal. <https://doi.org/10.48443/zr37-0238>
- NEON (National Ecological Observatory Network). (2022b). Chemical properties of surface water (DP1.20093.001), RELEASE-2022 [Dataset]. NEON Data Portal. <https://doi.org/10.48443/tx4b-zx50>
- NEON (National Ecological Observatory Network). (2022c). Continuous discharge (DP4.00130.001), RELEASE-2022 [Dataset]. NEON Data Portal. <https://doi.org/10.48443/xz4k-5j04>
- NEON (National Ecological Observatory Network). (2022d). Reaeration field and lab collection (DP1.20190.001), RELEASE-2022 [Dataset]. NEON Data Portal. <https://doi.org/10.48443/72cv-8c36>
- NEON (National Ecological Observatory Network). (2022e). Stream morphology map (DP4.00131.001), RELEASE-2022 [Dataset]. NEON Data Portal. <https://doi.org/10.48443/7px2-ve98>
- NEON (National Ecological Observatory Network). (2022f). Temperature at specific depth in surface water (DP1.20264.001), RELEASE-2022 [Dataset]. NEON Data Portal. <https://doi.org/10.48443/g7bs-7j57>
- NEON (National Ecological Observatory Network). (2022g). Temperature (PRT) in surface water (DP1.20053.001), RELEASE-2022 [Dataset]. NEON Data Portal. <https://doi.org/10.48443/m9et-tm58>
- NEON (National Ecological Observatory Network). (2022h). Water quality (DP1.20288.001), RELEASE-2022 [Dataset]. NEON Data Portal. <https://doi.org/10.48443/2ny7-q241>
- NEON (National Ecological Observatory Network). (2022i). Windspeed and direction above water on-buoy (DP1.20059.001), RELEASE-2022 [Dataset]. NEON Data Portal. <https://doi.org/10.48443/e16c-8686>
- Quick, A. M., Reeder, W. J., Farrell, T. B., Tonina, D., Feris, K. P., & Benner, S. G. (2019). Nitrous oxide from streams and rivers: A review of primary biogeochemical pathways and environmental variables. *Earth-Science Reviews*, *191*(February), 224–262. <https://doi.org/10.1016/j.earscirev.2019.02.021>
- Ravishankara, A. R., Daniel, J. S., & Portmann, R. W. (2009). Nitrous oxide (N₂O): The dominant ozone-depleting substance emitted in the 21st century. *Science*, *326*(5949), 123–125. <https://doi.org/10.1126/science.1176985>
- Raymond, P. A., Zappa, C. J., Butman, D., Bott, T. L., Potter, J., Mulholland, P., et al. (2012). Scaling the gas transfer velocity and hydraulic geometry in streams and small rivers. *Limnology and Oceanography: Fluids and Environments*, *2*(1), 41–53. <https://doi.org/10.1215/21573689-1597669>
- R Core Team. (2023). R: A language and environment for statistical computing [Software]. R Foundation for Statistical Computing. Retrieved from <https://www.gbif.org/tool/81287/r-a-language-and-environment-for-statistical-computing>
- Sander, R. (2015). Compilation of Henry's law constants (version 4.0) for water as solvent. *Atmospheric Chemistry and Physics*, *15*(8), 4399–4981. <https://doi.org/10.5194/acp-15-4399-2015>
- Seitzinger, S. P., & Kroeze, C. (1998). Global distribution of nitrous oxide production and N inputs in freshwater and coastal marine ecosystems. *Global Biogeochemical Cycles*, *12*(1), 93–113. <https://doi.org/10.1029/97GB03657>
- Soued, C., Del Giorgio, P. A., & Maranger, R. (2016). Nitrous oxide sinks and emissions in boreal aquatic networks in Quebec. *Nature Geoscience*, *9*(2), 116–120. <https://doi.org/10.1038/ngeo2611>
- Starry, O. S., Valett, H. M., & Schreiber, M. E. (2005). Nitrification rates in a headwater stream: Influences of seasonal variation in C and N supply. *Journal of the North American Benthological Society*, *24*(4), 753–768. <https://doi.org/10.1899/05-015.1>
- Stevens, R. J., & Laughlin, R. J. (1998). Measurement of nitrous oxide and di-nitrogen emissions from agricultural soils. *Nutrient Cycling in Agroecosystems*, *52*(2–3), 131–139. <https://doi.org/10.1023/a:1009715807023>
- Ulseth, A. J., Hall, R. O., Boix Canadell, M., Madinger, H. L., Niayifar, A., & Battin, T. J. (2019). Distinct air–water gas exchange regimes in low- and high-energy streams. *Nature Geoscience*, *12*(4), 259–263. <https://doi.org/10.1038/s41561-019-0324-8>
- Upstill-Goddard, R. C., Salter, M. E., Mann, P. J., Barnes, J., Poulsen, J., Dinga, B., et al. (2017). The riverine source of CH₄ and N₂O from the Republic of Congo, western Congo Basin. *Biogeosciences*, *14*(9), 2267–2281. <https://doi.org/10.5194/bg-14-2267-2017>
- Velthuis, M., & Veraart, A. J. (2022). Temperature sensitivity of freshwater denitrification and N₂O emission—A meta-analysis. *Global Biogeochemical Cycles*, *36*(6), 1–14. <https://doi.org/10.1029/2022GB007339>
- Wanninkhof, R. (1992). Relationship between wind speed and gas exchange over the ocean. *Journal of Geophysical Research*, *97*(C5), 7373–7382. <https://doi.org/10.1029/92JC00188>
- Webb, J. R., Hayes, N. M., Simpson, G. L., Leavitt, P. R., Baulch, H. M., & Finlay, K. (2019). Widespread nitrous oxide undersaturation in farm waterbodies creates an unexpected greenhouse gas sink. *Proceedings of the National Academy of Sciences of the United States of America*, *116*(20), 9814–9819. <https://doi.org/10.1073/pnas.1820389116>
- Winslow, L. A., Zwart, J. A., Batt, R. D., Dugan, H. A., Woolway, R. I., Corman, J. R., et al. (2016). LakeMetabolizer: An R package for estimating lake metabolism from free-water oxygen using diverse statistical models. *Inland Waters*, *6*(4), 622–636. <https://doi.org/10.1080/IW-6.4.883>
- Yao, Y., Tian, H., Shi, H., Pan, S., Xu, R., Pan, N., & Canadell, J. G. (2020). Increased global nitrous oxide emissions from streams and rivers in the Anthropocene. *Nature Climate Change*, *10*(2), 138–142. <https://doi.org/10.1038/s41558-019-0665-8>
- Yoshida, T., & Alexander, M. (1970). Nitrous oxide formation by Nitrosomonas europaea and hetero-trophic microorganisms. *Soil Science Society of America Proceedings*, *34*(6), 880–882. <https://doi.org/10.2136/sssaj1970.03615995003400060020x>
- Zhang, L., Zhang, S., Xia, X., Battin, T. J., Liu, S., Wang, Q., et al. (2022). Unexpectedly minor nitrous oxide emissions from fluvial networks draining permafrost catchments of the East Qinghai-Tibet Plateau. *Nature Communications*, *13*(1), 950. <https://doi.org/10.1038/s41467-022-28651-8>
- Zheng, Y., Wu, S., Xiao, S., Yu, K., Fang, X., Xia, L., et al. (2022). Global methane and nitrous oxide emissions from inland waters and estuaries. *Global Change Biology*, *28*(15), 4713–4725. <https://doi.org/10.1111/gcb.16233>

References From the Supporting Information

- Aho, K. S., & Raymond, P. A. (2019). Differential response of greenhouse gas evasion to storms in forested and wetland streams. *Journal of Geophysical Research: Biogeosciences*, *124*(3), 649–662. <https://doi.org/10.1029/2018jg004750>
- Koschorreck, M., Prairie, Y. T., Kim, J., & Marcé, R. (2021). Technical note: CO₂ is not like CH₄ – Limits of and corrections to the headspace method to analyse pCO₂ in fresh water. *Biogeosciences*, *18*(5), 1619–1627. <https://doi.org/10.5194/bg-18-1619-2021>
- Lewis, E., & Wallace, D. W. R. (1998). *Program developed for CO₂ system calculations* [Software]. ORNL/CDLAC-105.